Fermilab-Pub-09/006-E

Search for the standard model Higgs boson in diphoton final states with the D0 detector

V.M. Abazov[36], B. Abbott[75], M. Abolins[65], B.S. Acharya[29], M. Adams[51], T. Adams[49], E. Aguilo[6], M. Ahsan[59], G.D. Alexeev[36], G. Alkhazov[40], A. Alton[64,a], G. Alverson[63], G.A. Alves[2], M. Anastasoaie[35], L.S. Ancu[35], T. Andeen[53], B. Andrieu[17], M.S. Anzelc[53], M. Aoki[50], Y. Arnoud[14], M. Arov[60], M. Arthaud[18], A. Askew[49,b], B. Åsman[41], A.C.S. Assis Jesus[3], O. Atramentov[49], C. Avila[8], J. BackusMayes[82], F. Badaud[13], L. Bagby[50], B. Baldin[50], D.V. Bandurin[59], P. Banerjee[29], S. Banerjee[29], E. Barberis[63], A.-F. Barfuss[15], P. Bargassa[80], P. Baringer[58], J. Barreto[2], J.F. Bartlett[50], U. Bassler[18], D. Bauer[43], S. Beale[6], A. Bean[58], M. Begalli[3], M. Begel[73], C. Belanger-Champagne[41], L. Bellantoni[50], A. Bellavance[50], J.A. Benitez[65], S.B. Beri[27], G. Bernardi[17], R. Bernhard[23], I. Bertram[42], M. Besançon[18], R. Beuselinck[43], V.A. Bezzubov[39], P.C. Bhat[50], V. Bhatnagar[27], G. Blazey[52], F. Blekman[43], S. Blessing[49], K. Bloom[67], A. Boehnlein[50], D. Boline[62], T.A. Bolton[59], E.E. Boos[38], G. Borissov[42], T. Bose[77], A. Brandt[78], R. Brock[65], G. Brooijmans[70], A. Bross[50], D. Brown[19], X.B. Bu[7], N.J. Buchanan[49], D. Buchholz[53], M. Buehler[81], V. Buescher[22], V. Bunichev[38], S. Burdin[42,c], T.H. Burnett[82], C.P. Buszello[43], P. Calfayan[25], B. Calpas[15], S. Calvet[16], J. Cammin[71], M.A. Carrasco-Lizarraga[33], E. Carrera[49], W. Carvalho[3], B.C.K. Casey[50], H. Castilla-Valdez[33], S. Chakrabarti[72], D. Chakraborty[52], K.M. Chan[55], A. Chandra[48], E. Cheu[45], D.K. Cho[62], S. Choi[32], B. Choudhary[28], L. Christofek[77], T. Christoudias[43], S. Cihangir[50], D. Claes[67], J. Clutter[58], M. Cooke[50], W.E. Cooper[50], M. Corcoran[80], F. Couderc[18], M.-C. Cousinou[15], S. Crépé-Renaudin[14], V. Cuplov[59], D. Cutts[77], M. Ćwiok[30], H. da Motta[2], A. Das[45], G. Davies[43], K. De[78], S.J. de Jong[35], E. De La Cruz-Burelo[33], C. De Oliveira Martins[3], K. DeVaughan[67], F. Déliot[18], M. Demarteau[50], R. Demina[71], D. Denisov[50], S.P. Denisov[39], S. Desai[50], H.T. Diehl[50], M. Diesburg[50], A. Dominguez[67], T. Dorland[82], A. Dubey[28], L.V. Dudko[38], L. Duflot[16], S.R. Dugad[29], D. Duggan[49], A. Duperrin[15], S. Dutt[27], J. Dyer[65], A. Dyshkant[52], M. Eads[67], D. Edmunds[65], J. Ellison[48], V.D. Elvira[50], Y. Enari[77], S. Eno[61], P. Ermolov[38,‡], M. Escalier[15], H. Evans[54], A. Evdokimov[73], V.N. Evdokimov[39], A.V. Ferapontov[59], T. Ferbel[61,71], F. Fiedler[24], F. Filthaut[35], W. Fisher[50], H.E. Fisk[50], M. Fortner[52], H. Fox[42], S. Fu[50], S. Fuess[50], T. Gadfort[70], C.F. Galea[35], C. Garcia[71], A. Garcia-Bellido[71], V. Gavrilov[37], P. Gay[13], W. Geist[19], W. Geng[15,65], C.E. Gerber[51], Y. Gershtein[49,b], D. Gillberg[6], G. Ginther[71], B. Gómez[8], A. Goussiou[82], P.D. Grannis[72], H. Greenlee[50], Z.D. Greenwood[60], E.M. Gregores[4], G. Grenier[20], Ph. Gris[13], J.-F. Grivaz[16], A. Grohsjean[25], S. Grünendahl[50], M.W. Grünewald[30], F. Guo[72], J. Guo[72], G. Gutierrez[50], P. Gutierrez[75], A. Haas[70], N.J. Hadley[61], P. Haefner[25], S. Hagopian[49], J. Haley[68], I. Hall[65], R.E. Hall[47], L. Han[7], K. Harder[44], A. Harel[71], J.M. Hauptman[57], J. Hays[43], T. Hebbeker[21], D. Hedin[52], J.G. Hegeman[34], A.P. Heinson[48], U. Heintz[62], C. Hensel[22,d], K. Herner[72], G. Hesketh[63], M.D. Hildreth[55], R. Hirosky[81], T. Hoang[49], J.D. Hobbs[72], B. Hoeneisen[12], M. Hohlfeld[22], S. Hossain[75], P. Houben[34], Y. Hu[72], Z. Hubacek[10], N. Huske[17], V. Hynek[9], I. Iashvili[69], R. Illingworth[50], A.S. Ito[50], S. Jabeen[62], M. Jaffré[16], S. Jain[75], K. Jakobs[23], C. Jarvis[61], R. Jesik[43], K. Johns[45], C. Johnson[70], M. Johnson[50], D. Johnston[67], A. Jonckheere[50], P. Jonsson[43], A. Juste[50], E. Kajfasz[15], D. Karmanov[38], P.A. Kasper[50], I. Katsanos[70], V. Kaushik[78], R. Kehoe[79], S. Kermiche[15], N. Khalatyan[50], A. Khanov[76], A. Kharchilava[69], Y.N. Kharzheev[36], D. Khatidze[70], T.J. Kim[31], M.H. Kirby[53], M. Kirsch[21], B. Klima[50], J.M. Kohli[27], J.-P. Konrath[23], A.V. Kozelov[39], J. Kraus[65], T. Kuhl[24], A. Kumar[69], A. Kupco[11], T. Kurča[20], V.A. Kuzmin[38], J. Kvita[9], F. Lacroix[13], D. Lam[55], S. Lammers[70], G. Landsberg[77], P. Lebrun[20], W.M. Lee[50], A. Leflat[38], J. Lellouch[17], J. Li[78,‡], L. Li[48], Q.Z. Li[50], S.M. Lietti[5], J.K. Lim[31], J.G.R. Lima[52], D. Lincoln[50], J. Linnemann[65], V.V. Lipaev[39], R. Lipton[50], Y. Liu[7], Z. Liu[6], A. Lobodenko[40], M. Lokajicek[11], P. Love[42], H.J. Lubatti[82], R. Luna-Garcia[33,e], A.L. Lyon[50], A.K.A. Maciel[2], D. Mackin[80], R.J. Madaras[46], P. Mättig[26], A. Magerkurth[64], P.K. Mal[82], H.B. Malbouisson[3], S. Malik[67], V.L. Malyshev[36], Y. Maravin[59], B. Martin[14], R. McCarthy[72], M.M. Meijer[35], A. Melnitchouk[66], L. Mendoza[8], P.G. Mercadante[5], M. Merkin[38], K.W. Merritt[50], A. Meyer[21], J. Meyer[22,d], J. Mitrevski[70], R.K. Mommsen[44], N.K. Mondal[29], R.W. Moore[6], T. Moulik[58], G.S. Muanza[15], M. Mulhearn[70], O. Mundal[22], L. Mundim[3], E. Nagy[15], M. Naimuddin[50], M. Narain[77], H.A. Neal[64], J.P. Negret[8], P. Neustroev[40], H. Nilsen[23], H. Nogima[3], S.F. Novaes[5], T. Nunnemann[25], D.C. O'Neil[6], G. Obrant[40], C. Ochando[16], D. Onoprienko[59], N. Oshima[50], N. Osman[43], J. Osta[55], R. Otec[10], G.J. Otero y Garzón[1], M. Owen[44], M. Padilla[48], P. Padley[80], M. Pangilinan[77], N. Parashar[56], S.-J. Park[22,d], S.K. Park[31], J. Parsons[70], R. Partridge[77], N. Parua[54], A. Patwa[73], G. Pawloski[80], B. Penning[23], M. Perfilov[38], K. Peters[44], Y. Peters[26], P. Pétroff[16], M. Petteni[43], R. Piegaia[1], J. Piper[65], M.-A. Pleier[22],

P.L.M. Podesta-Lerma[33,f], V.M. Podstavkov[50], Y. Pogorelov[55], M.-E. Pol[2], P. Polozov[37], B.G. Pope[65], A.V. Popov[39], C. Potter[6], W.L. Prado da Silva[3], H.B. Prosper[49], S. Protopopescu[73], J. Qian[64], A. Quadt[22,d], B. Quinn[66], A. Rakitine[42], M.S. Rangel[2], K. Ranjan[28], P.N. Ratoff[42], P. Renkel[79], P. Rich[44], M. Rijssenbeek[72], I. Ripp-Baudot[19], F. Rizatdinova[76], S. Robinson[43], R.F. Rodrigues[3], M. Rominsky[75], C. Royon[18], P. Rubinov[50], R. Ruchti[55], G. Safronov[37], G. Sajot[14], A. Sánchez-Hernández[33], M.P. Sanders[17], B. Sanghi[50], G. Savage[50], L. Sawyer[60], T. Scanlon[43], D. Schaile[25], R.D. Schamberger[72], Y. Scheglov[40], H. Schellman[53], T. Schliephake[26], S. Schlobohm[82], C. Schwanenberger[44], R. Schwienhorst[65], J. Sekaric[49], H. Severini[75], E. Shabalina[51], M. Shamim[59], V. Shary[18], A.A. Shchukin[39], R.K. Shivpuri[28], V. Siccardi[19], V. Simak[10], V. Sirotenko[50], P. Skubic[75], P. Slattery[71], D. Smirnov[55], G.R. Snow[67], J. Snow[74], S. Snyder[73], S. Söldner-Rembold[44], L. Sonnenschein[17], A. Sopczak[42], M. Sosebee[78], K. Soustruznik[9], B. Spurlock[78], J. Stark[14], V. Stolin[37], D.A. Stoyanova[39], J. Strandberg[64], S. Strandberg[41], M.A. Strang[69], E. Strauss[72], M. Strauss[75], R. Ströhmer[25], D. Strom[53], L. Stutte[50], S. Sumowidagdo[49], P. Svoisky[35], A. Sznajder[3], A. Tanasijczuk[1], W. Taylor[6], B. Tiller[25], F. Tissandier[13], M. Titov[18], V.V. Tokmenin[36], I. Torchiani[23], D. Tsybychev[72], B. Tuchming[18], C. Tully[68], P.M. Tuts[70], R. Unalan[65], L. Uvarov[40], S. Uvarov[40], S. Uzunyan[52], B. Vachon[6], P.J. van den Berg[34], R. Van Kooten[54], W.M. van Leeuwen[34], N. Varelas[51], E.W. Varnes[45], I.A. Vasilyev[39], P. Verdier[20], L.S. Vertogradov[36], M. Verzocchi[50], D. Vilanova[18], F. Villeneuve-Seguier[43], P. Vint[43], P. Vokac[10], M. Voutilainen[67,g], R. Wagner[68], H.D. Wahl[49], M.H.L.S. Wang[50], J. Warchol[55], G. Watts[82], M. Wayne[55], G. Weber[24], M. Weber[50,h], L. Welty-Rieger[54], A. Wenger[23,i], N. Wermes[22], M. Wetstein[61], A. White[78], D. Wicke[26], M.R.J. Williams[42], G.W. Wilson[58], S.J. Wimpenny[48], M. Wobisch[60], D.R. Wood[63], T.R. Wyatt[44], Y. Xie[77], C. Xu[64], S. Yacoob[53], R. Yamada[50], W.-C. Yang[44], T. Yasuda[50], Y.A. Yatsunenko[36], Z. Ye[50], H. Yin[7], K. Yip[73], H.D. Yoo[77], S.W. Youn[53], J. Yu[78], C. Zeitnitz[26], S. Zelitch[81], T. Zhao[82], B. Zhou[64], J. Zhu[72], M. Zielinski[71], D. Zieminska[54], L. Zivkovic[70], V. Zutshi[52], and E.G. Zverev[38]

(The DØ Collaboration)

[1] *Universidad de Buenos Aires, Buenos Aires, Argentina*
[2] *LAFEX, Centro Brasileiro de Pesquisas Físicas, Rio de Janeiro, Brazil*
[3] *Universidade do Estado do Rio de Janeiro, Rio de Janeiro, Brazil*
[4] *Universidade Federal do ABC, Santo André, Brazil*
[5] *Instituto de Física Teórica, Universidade Estadual Paulista, São Paulo, Brazil*
[6] *University of Alberta, Edmonton, Alberta, Canada, Simon Fraser University, Burnaby, British Columbia, Canada, York University, Toronto, Ontario, Canada, and McGill University, Montreal, Quebec, Canada*
[7] *University of Science and Technology of China, Hefei, People's Republic of China*
[8] *Universidad de los Andes, Bogotá, Colombia*
[9] *Center for Particle Physics, Charles University, Prague, Czech Republic*
[10] *Czech Technical University, Prague, Czech Republic*
[11] *Center for Particle Physics, Institute of Physics, Academy of Sciences of the Czech Republic, Prague, Czech Republic*
[12] *Universidad San Francisco de Quito, Quito, Ecuador*
[13] *LPC, Université Blaise Pascal, CNRS/IN2P3, Clermont, France*
[14] *LPSC, Université Joseph Fourier Grenoble 1, CNRS/IN2P3, Institut National Polytechnique de Grenoble, Grenoble, France*
[15] *CPPM, Aix-Marseille Université, CNRS/IN2P3, Marseille, France*
[16] *LAL, Université Paris-Sud, IN2P3/CNRS, Orsay, France*
[17] *LPNHE, IN2P3/CNRS, Universités Paris VI and VII, Paris, France*
[18] *CEA, Irfu, SPP, Saclay, France*
[19] *IPHC, Université Louis Pasteur, CNRS/IN2P3, Strasbourg, France*
[20] *IPNL, Université Lyon 1, CNRS/IN2P3, Villeurbanne, France and Université de Lyon, Lyon, France*
[21] *III. Physikalisches Institut A, RWTH Aachen University, Aachen, Germany*
[22] *Physikalisches Institut, Universität Bonn, Bonn, Germany*
[23] *Physikalisches Institut, Universität Freiburg, Freiburg, Germany*
[24] *Institut für Physik, Universität Mainz, Mainz, Germany*
[25] *Ludwig-Maximilians-Universität München, München, Germany*
[26] *Fachbereich Physik, University of Wuppertal, Wuppertal, Germany*
[27] *Panjab University, Chandigarh, India*
[28] *Delhi University, Delhi, India*
[29] *Tata Institute of Fundamental Research, Mumbai, India*
[30] *University College Dublin, Dublin, Ireland*

[31] *Korea Detector Laboratory, Korea University, Seoul, Korea*
[32] *SungKyunKwan University, Suwon, Korea*
[33] *CINVESTAV, Mexico City, Mexico*
[34] *FOM-Institute NIKHEF and University of Amsterdam/NIKHEF, Amsterdam, The Netherlands*
[35] *Radboud University Nijmegen/NIKHEF, Nijmegen, The Netherlands*
[36] *Joint Institute for Nuclear Research, Dubna, Russia*
[37] *Institute for Theoretical and Experimental Physics, Moscow, Russia*
[38] *Moscow State University, Moscow, Russia*
[39] *Institute for High Energy Physics, Protvino, Russia*
[40] *Petersburg Nuclear Physics Institute, St. Petersburg, Russia*
[41] *Lund University, Lund, Sweden, Royal Institute of Technology and Stockholm University, Stockholm, Sweden, and Uppsala University, Uppsala, Sweden*
[42] *Lancaster University, Lancaster, United Kingdom*
[43] *Imperial College, London, United Kingdom*
[44] *University of Manchester, Manchester, United Kingdom*
[45] *University of Arizona, Tucson, Arizona 85721, USA*
[46] *Lawrence Berkeley National Laboratory and University of California, Berkeley, California 94720, USA*
[47] *California State University, Fresno, California 93740, USA*
[48] *University of California, Riverside, California 92521, USA*
[49] *Florida State University, Tallahassee, Florida 32306, USA*
[50] *Fermi National Accelerator Laboratory, Batavia, Illinois 60510, USA*
[51] *University of Illinois at Chicago, Chicago, Illinois 60607, USA*
[52] *Northern Illinois University, DeKalb, Illinois 60115, USA*
[53] *Northwestern University, Evanston, Illinois 60208, USA*
[54] *Indiana University, Bloomington, Indiana 47405, USA*
[55] *University of Notre Dame, Notre Dame, Indiana 46556, USA*
[56] *Purdue University Calumet, Hammond, Indiana 46323, USA*
[57] *Iowa State University, Ames, Iowa 50011, USA*
[58] *University of Kansas, Lawrence, Kansas 66045, USA*
[59] *Kansas State University, Manhattan, Kansas 66506, USA*
[60] *Louisiana Tech University, Ruston, Louisiana 71272, USA*
[61] *University of Maryland, College Park, Maryland 20742, USA*
[62] *Boston University, Boston, Massachusetts 02215, USA*
[63] *Northeastern University, Boston, Massachusetts 02115, USA*
[64] *University of Michigan, Ann Arbor, Michigan 48109, USA*
[65] *Michigan State University, East Lansing, Michigan 48824, USA*
[66] *University of Mississippi, University, Mississippi 38677, USA*
[67] *University of Nebraska, Lincoln, Nebraska 68588, USA*
[68] *Princeton University, Princeton, New Jersey 08544, USA*
[69] *State University of New York, Buffalo, New York 14260, USA*
[70] *Columbia University, New York, New York 10027, USA*
[71] *University of Rochester, Rochester, New York 14627, USA*
[72] *State University of New York, Stony Brook, New York 11794, USA*
[73] *Brookhaven National Laboratory, Upton, New York 11973, USA*
[74] *Langston University, Langston, Oklahoma 73050, USA*
[75] *University of Oklahoma, Norman, Oklahoma 73019, USA*
[76] *Oklahoma State University, Stillwater, Oklahoma 74078, USA*
[77] *Brown University, Providence, Rhode Island 02912, USA*
[78] *University of Texas, Arlington, Texas 76019, USA*
[79] *Southern Methodist University, Dallas, Texas 75275, USA*
[80] *Rice University, Houston, Texas 77005, USA*
[81] *University of Virginia, Charlottesville, Virginia 22901, USA and*
[82] *University of Washington, Seattle, Washington 98195, USA*

(Dated: January 13, 2009)

We present a search for the standard model Higgs boson in the inclusive diphoton final state using ~ 2.7 fb^{-1} of data collected with the D0 detector at the Fermilab Tevatron $p\bar{p}$ Collider. We observe good agreement between the data and the background prediction, and set 95% C.L. upper limits on the Higgs production cross section times the branching ratio for $H \to \gamma\gamma$ for Higgs boson masses between 100 and 150 GeV. For a Higgs boson mass of 130 GeV, we obtain an observed (expected) limit of 41.9 (49.1) fb, a factor of 18.7 (21.9) above the standard model prediction.

PACS numbers: 14.80.Bn, 13.85.Rm, 13.85.Qk

In the standard model (SM), the Higgs boson, a fundamental scalar still awaiting experimental verification, is the agent responsible for the spontaneous breaking of the electroweak symmetry and the generation of the mass of particles. The combination of direct searches at the CERN LEP Collider [1] and indirect constraints from precision electroweak measurements yields a preferred range for the SM Higgs boson mass (M_H) of $114.4 < M_H < 185$ GeV at 95% C.L. [2]. The dominant SM Higgs boson production mechanisms in $p\bar{p}$ collisions at $\sqrt{s} = 1.96$ TeV are gluon fusion ($gg \to H$), associated production with a W or Z boson ($q\bar{q}' \to VH$, $V = W, Z$), and vector boson fusion ($VV \to H$, or VBF). The most sensitive SM Higgs boson searches at the Fermilab Tevatron Collider are being performed in the $VH(\to b\bar{b})$ and $gg \to H(\to WW^{(*)})$ channels, achieving similar sensitivity at $M_H \sim 125$ GeV [3], but quickly degrading at higher and lower M_H, respectively. To increase the overall sensitivity in the intermediate mass region, $125 < M_H < 145$ GeV, as well as the model independence of the search, it is important to consider additional Higgs boson production and decay modes. One such mode is $H \to \gamma\gamma$ which, despite the small SM branching ratio of $\sim 0.2\%$ for $110 < M_H < 140$ GeV, is considered to be one of the most promising discovery channels at hadron colliders due to its clean signature of a narrow resonance in the diphoton mass spectrum over a steeply falling background. Furthermore, in some models beyond the SM [4], the $H \to \gamma\gamma$ branching ratio can be enhanced significantly relative to the SM prediction. Thus, observing a significant excess in this channel would point to a non-SM Higgs sector. In particular, scenarios with a fermiophobic Higgs boson have been tested at LEP and the Tevatron [5].

In this Letter, we present the result of a quasi model-independent search for a resonance in the diphoton mass spectrum using a data sample collected by the D0 detector at the Fermilab Tevatron Collider. The result of this search is interpreted in the context of the SM Higgs boson, representing the first SM Higgs boson search in this channel at the Tevatron and making this analysis a forerunner to similar planned searches at the LHC [6].

The subdetectors most relevant to this analysis are: the central tracking system, composed of a silicon microstrip tracker (SMT) and a central fiber tracker (CFT) embedded in a 2 T solenoidal magnetic field, the central preshower (CPS), and the liquid-argon/uranium sampling calorimeter. The CPS is located immediately before the inner layer of the calorimeter and is formed of one radiation length of absorber followed by several layers of scintillating strips. The calorimeter consists of a central section with coverage of $|\eta| < 1.1$ [8], and two end calorimeters covering up to $|\eta| \simeq 4.2$. The electromagnetic (EM) section of the calorimeter is segmented into four longitudinal layers with transverse segmentation of $\Delta\eta \times \Delta\phi = 0.1 \times 0.1$ [8], except in the third layer (EM3), where it is 0.05×0.05. The data used in this analysis were collected using triggers requiring at least two clusters of energy in the EM calorimeter and correspond to an integrated luminosity of 2.7 ± 0.2 fb^{-1} [9].

Events are selected by requiring at least two photon candidates with transverse momentum $p_T > 25$ GeV and $|\eta| < 1.1$, for which the trigger requirements are fully efficient. Photons are selected from EM clusters reconstructed within a cone with radius $\mathcal{R} = \sqrt{(\Delta\eta)^2 + (\Delta\phi)^2} = 0.2$ by requiring: $\geq 97\%$ of the cluster energy is deposited in the EM calorimeter, (ii) the calorimeter isolation variable $I = [E_{\rm tot}(0.4) - E_{\rm EM}(0.2)]/E_{\rm EM}(0.2) < 0.1$, where $E_{\rm tot}(\mathcal{R})$ ($E_{\rm EM}(\mathcal{R})$) is the total (EM) energy in a cone of radius $\mathcal{R}$; (iii) the energy-weighted shower width in the $r-\phi$ plane in EM3 is $< \sqrt{14}$ cm; and (iv) the scalar sum of the p_T of all tracks ($p_{T\rm trk}^{\rm sum}$) originating from the primary vertex in an annulus of $0.05 < \mathcal{R} < 0.4$ around the cluster is < 2 GeV. To suppress electrons misidentified as photons, the EM clusters are required to not be spatially matched to tracker activity, either a reconstructed track, or a density of hits in the SMT and CFT consistent with that of an electron [10]. To suppress jets misidentified as photons, a neural network (NN) [11] is trained using a set of variables sensitive to differences between photons and jets in the tracker activity and in the energy distributions in the calorimeter and CPS: $p_{T\rm trk}^{\rm sum}$, the numbers of cells above threshold in the first EM calorimeter layer within $\mathcal{R} < 0.2$ and $0.2 < \mathcal{R} < 0.4$ of the EM cluster, the number of CPS clusters within $\mathcal{R} < 0.1$ of the EM cluster, and the squared-energy-weighted width of the energy deposit in the CPS. The NN is trained using diphoton and dijet Monte Carlo (MC) samples and its performance is verified using a data sample of $Z \to \ell^+\ell^-\gamma$ ($\ell = e, \mu$) events. Fig. 1a compares the NN output (O_{NN}) spectrum for photons and jets. Photon candidates are required to have $O_{NN} > 0.1$, which is $\sim 98\%$ efficient for real photons and rejects $\sim 50\%$ of misidentified jets. Finally, the diphoton mass ($M_{\gamma\gamma}$), computed from the two highest p_T photons, is required to be > 60 GeV. After all requirements, a total of 5608 events are selected in data.

All MC samples used in this analysis are generated using PYTHIA [12] with CTEQ6L [13] parton distribution functions (PDFs), and processed through a GEANT-based [14] simulation of the D0 detector and the same reconstruction software as the data. Samples corresponding to each of the three dominant SM Higgs boson production mechanisms discussed above are generated, and normalized using the next-to-next-to-leading order (NNLO) theoretical cross sections [15–17] and branching ratio predictions from HDECAY [18].

This analysis is affected by instrumental backgrounds such as γ+jet, dijet and $Z/\gamma^* \to e^+e^-$ production, with jets or electrons misidentified as photons, as well as an irreducible background from direct diphoton production (DDP). All backgrounds, except for $Z/\gamma^* \to e^+e^-$, are

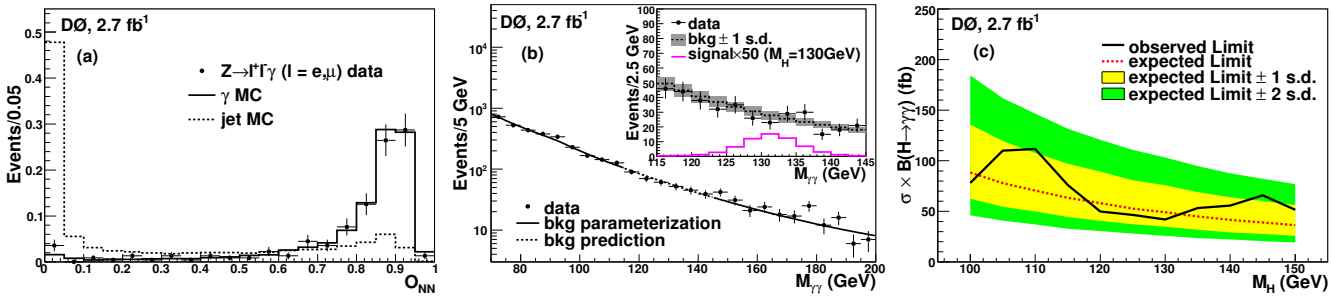

FIG. 1: (a) Normalized O_{NN} spectrum for photons and jets. (b) $M_{\gamma\gamma}$ spectrum in data (points) compared to the total background parameterization (solid line) including the DDP contribution derived via side-band fitting, and the total background prediction (dashed line) inside the search region for $M_H = 130$ GeV. The inset figure compares the data to the total background prediction inside the search region including its one standard deviation (s.d.) uncertainty band, as well as the expected signal scaled by a factor of 50. (c) Observed and expected 95% C.L. upper limits on $\sigma \times B$ as a function of M_H. The one and two s.d. bands on the expected limits are also shown.

estimated directly from data.

The $Z/\gamma^* \to e^+e^-$ background is estimated using the MC simulation, normalized to the NNLO cross section [19]. To improve the agreement between data and simulation, selection efficiencies determined by the MC are corrected to the corresponding values measured in the data. On average each electron has a 2% probability to satisfy the photon selection criteria, mainly due to the inefficiency of the track-match veto requirements. The total contribution from $Z/\gamma^* \to e^+e^-$ is estimated to be 88 ± 10 events, mainly located around the Z pole.

Backgrounds due to γ+jet and dijet events are directly estimated from data by using a 4×4 matrix background estimation method [20]. After final event selection, a tightened O_{NN} requirement ($O_{NN} > 0.75$) is used to classify the events into four categories depending on whether the two highest-p_T photons, only the leading photon, only the trailing photon or neither of the two photons, satisfy this requirement. The corresponding numbers of events, after subtraction of the estimated $Z/\gamma^* \to e^+e^-$ contributions, are denoted as N_{pp}, N_{pf}, N_{fp} and N_{ff}. The different relative efficiency of the $O_{NN} > 0.75$ requirement between real photons and jets allows the estimation of the sample composition by solving a linear system of equations: $(N_{pp}, N_{pf}, N_{fp}, N_{ff}) = \mathcal{E} \times (N_{\gamma\gamma}, N_{\gamma j}, N_{j\gamma}, N_{jj})$, where $N_{\gamma\gamma}$ (N_{jj}) is the number of $\gamma\gamma$ (dijet) events and $N_{\gamma j}$ ($N_{j\gamma}$) is the number of γ+jet events with the leading (trailing) cluster as the photon. The 4×4 matrix $\mathcal{E}$ contains the efficiency terms (parameterized as a function of $|\eta|$), estimated in photon and jet MC samples and validated in data. The estimated sample composition is $N_{\gamma\gamma} = 3155 \pm 125$ (stat.), $N_{\gamma j + j\gamma} = 1680 \pm 149$ (stat.) and $N_{jj} = 685 \pm 93$ (stat.). The shape of the $M_{\gamma\gamma}$ spectrum for the sum of the γ+jet and dijet backgrounds is obtained from an independent control data sample by requiring $O_{NN} < 0.1$ for one of the photon candidates, and is parameterized with an exponential function. The resulting shape is found to be in excellent agreement with that derived by directly applying the 4×4 matrix method bin-by-bin in the final selected sample, but has smaller statistical fluctuations, especially in the high $M_{\gamma\gamma}$ region.

After subtraction of the $Z/\gamma^* \to e^+e^-$, γ+jet and dijet background contributions, the $M_{\gamma\gamma}$ spectrum is examined for the presence of a narrow resonance. For each assumed M_H value (between 100 and 150 GeV, in steps of 5 GeV), the search region is defined to be $(M_H - 15$ GeV, $M_H + 15$ GeV), where 15 GeV corresponds to about five times the expected $M_{\gamma\gamma}$ resolution. The DDP background is estimated by performing a side-band fit to the $M_{\gamma\gamma}$ spectrum in the $(70, 200)$ GeV range (this excludes the search region) using an exponential function (see Fig. 1b). Such a parameterization has been validated using a NLO calculation for this process [21].

Systematic uncertainties affecting the normalization and shape of the $M_{\gamma\gamma}$ spectrum are estimated for both signal and backgrounds. Uncertainties affecting the $Z/\gamma^* \to e^+e^-$ background normalization include: integrated luminosity (6.1%), electron misidentification rate (14.3%) and $Z/\gamma^* \to e^+e^-$ cross section (3.9%). Such uncertainties are propagated, via the 4×4 matrix method, to the estimated normalization of the γ+jet and dijet background contributions, affected in addition by the uncertainty on the $O_{NN} > 0.75$ selection efficiency for photons (2%) and jets (10%). The uncertainty in the shape of the γ+jet and dijet $M_{\gamma\gamma}$ spectrum is given by the statistics of the control data sample used to parameterize it. The above uncertainties, as well as the statistical uncertainties of the side-band fitting method, result in systematic uncertainties in the normalization and shape of the DDP background contribution. Uncertainties affecting the signal normalization include uncertainties in the integrated luminosity (6.1%) and acceptance due to the photon identification efficiency (6.8%) and the PDFs (1.7-2.2%). Finally, the location of the peak in the $M_{\gamma\gamma}$ spectrum for signal is affected by the uncertainty in

M_H (GeV)	100	110	120	130	140	150
$Z/\gamma^* \to e^+e^-$	55±7	17±3	6±2	5±1	4±1	3±1
$\gamma\gamma$	742±62	481±42	324±34	236±30	161±28	124±22
$\gamma j + jj$	540±66	319±39	204±25	133±16	89±11	61±8
total background	1337±29	817±26	534±19	374±12	254±7	188±5
data	1385	827	544	357	270	202
signal	1.62±0.11	1.61±0.11	1.51±0.10	1.26±0.08	0.90±0.06	0.54±0.04
acceptance (%)	19.9/18.8/20.3	20.4/19.9/21.6	21.0/20.6/22.3	21.5/21.2/22.9	21.8/22.0/23.5	22.1/22.2/24.1

TABLE I: Numbers of selected events in data, expected backgrounds, expected signal and signal acceptance (for each production mechanism: gluon fusion/VH/VBF), in the search region for different M_H values. The expected signal includes contributions from gluon fusion, VH and VBF processes, the two latter representing $\sim 21-24\%$ of the total signal.

M_H (GeV)	100	105	110	115	120	125	130	135	140	145	150
exp. $\sigma \times B$	88.4	77.8	70.6	63.3	58.1	52.7	49.1	45.0	41.2	39.0	36.4
obs. $\sigma \times B$	78.0	109.9	111.6	75.9	49.8	46.4	41.9	53.3	55.7	65.9	51.6
exp. ratio	28.0	25.0	23.2	21.7	21.1	20.9	21.9	23.5	26.3	31.4	39.3
obs. ratio	24.7	35.3	36.7	26.0	18.1	18.4	18.7	27.8	35.2	53.0	55.7

TABLE II: Observed and expected 95% C.L. upper limits on $\sigma \times B$ (in fb) for different M_H values. The corresponding ratios to the predicted SM cross section are also given.

the relative photon energy scale between data and MC (0.6%).

Table I shows the number of events in data, expected background and expected signal in six different search regions. The inset in Fig. 1b illustrates the $M_{\gamma\gamma}$ spectrum in the search region for $M_H = 130$ GeV, found to be in good agreement with the background prediction. The $M_{\gamma\gamma}$ spectrum in the search region is used to derive upper limits on the production cross section times branching ratio for $H \to \gamma\gamma$ ($\sigma \times B$) as a function of M_H. The SM prediction for the ratio of the production cross sections for the three signal production mechanisms is assumed. However, despite the different event signature for each of the signal processes, the use of the $M_{\gamma\gamma}$ spectrum as the main observable, and the very similar signal acceptance (see Table I), makes the estimated limits quasi model independent. Limits are calculated at the 95% C.L. using the modified frequentist approach with a Poisson log-likelihood ratio test statistic [23, 24]. The impact of systematic uncertainties is incorporated via convolution of the Poisson probability distributions for signal and background with Gaussian distributions corresponding to the different sources of systematic uncertainty. The correlations in systematic uncertainties are maintained between signal and backgrounds. The resulting limits on $\sigma \times B$ are displayed in Fig. 1c and given in Table II. The expected limit is defined as the median of the distribution of limits in background-only pseudo-experiments. For $M_H = 130$ GeV, the observed (expected) limit is 41.9 (49.1) fb, a factor of 18.7 (21.9) larger than the SM prediction. Compared to Ref. [5], the expected sensitivity to a fermiophobic Higgs boson is improved by $\sim 13-40\%$, depending on M_H, with increased model independence.

In summary, we have presented the first 95% C.L. upper limits at the Tevatron on the production cross section times branching ratio for $H \to \gamma\gamma$ for Higgs boson masses in the $100 < M_H < 150$ GeV range. This search helps to increase the overall sensitivity of the SM Higgs boson search program at the Tevatron and allows the probe of new physics models predicting an enhanced rate for $H \to \gamma\gamma$.

We thank the staffs at Fermilab and collaborating institutions, and acknowledge support from the DOE and NSF (USA); CEA and CNRS/IN2P3 (France); FASI, Rosatom and RFBR (Russia); CNPq, FAPERJ, FAPESP and FUNDUNESP (Brazil); DAE and DST (India); Colciencias (Colombia); CONACyT (Mexico); KRF and KOSEF (Korea); CONICET and UBACyT (Argentina); FOM (The Netherlands); STFC (United Kingdom); MSMT and GACR (Czech Republic); CRC Program, CFI, NSERC and WestGrid Project (Canada); BMBF and DFG (Germany); SFI (Ireland); The Swedish Research Council (Sweden); CAS and CNSF (China); and the Alexander von Humboldt Foundation (Germany).

[a] Visitor from Augustana College, Sioux Falls, SD, USA.
[b] Visitor from Rutgers University, Piscataway, NJ, USA.
[c] Visitor from The University of Liverpool, Liverpool, UK.
[d] Visitor from II. Physikalisches Institut, Georg-August-University, Göttingen, Germany.
[e] Visitor from Centro de Investigacion en Computacion - IPN, Mexico City, Mexico.
[f] Visitor from ECFM, Universidad Autonoma de Sinaloa, Culiacán, Mexico.
[g] Visitor from Helsinki Institute of Physics, Helsinki, Finland.
[h] Visitor from Universität Bern, Bern, Switzerland.
[i] Visitor from Universität Zürich, Zürich, Switzerland.
[‡] Deceased.

[1] R. Barate *et al.*, Phys. Lett. B **365**, 61 (2003).
[2] The ALEPH, CDF, D0, DELPHI, L3, OPAL, SLD Collaborations, the LEP Electroweak Working Group, the Tevatron Electroweak Working Group, and the SLD elec-

troweak and heavy flavour groups, arXiv:0811.4682 [hep-ex] (2008).
[3] The TEVNPH Working Group, for the CDF and D0 Collaborations, arXiv:0804.3423 [hep-ex] (2008); arXiv:0808.0534 [hep-ex] (2008); and references therein.
[4] S. Mrenna and J. Wells, Phys. Rev. D **63**, 015006 (2001).
[5] V.M. Abazov *et al.* (D0 Collaboration), Phys. Rev. Lett. **101**, 051801 (2008); and references therein.
[6] ATLAS Collaboration, CERN/LHCC 1999-15 (1999); L. Carminati, Acta Phys. Polon. B **38**, 747 (2007); CMS Collaboration, CERN/LHCC 2006-021 (2006).
[7] V.M. Abazov *et al.* (D0 Collaboration), Nucl. Instrum. Methods Phys. Res., Sect. A **565**, 463 (2006).
[8] Pseudorapidity is defined as $\eta = -\ln[\tan(\theta/2)]$, where θ is the polar angle relative to the proton beam direction. ϕ is defined as the azimuthal angle in the plane transverse to the proton beam direction.
[9] T. Andeen *et al.*, FERMILAB-TM-2365 (2007).
[10] V.M. Abazov *et al.*, (D0 Collaboration), Phys. Lett. B **659**, 856 (2008).
[11] C. Peterson, T. Rognvaldsson and L. Lönnblad, Comput. Phys. Commun. **81**, 15 (1994).
[12] T. Sjöstrand *et al.*, Comput. Phys. Commun. **135**, 238 (2001).
[13] H.L. Lai *et al.*, Phys. Rev. D **55**, 1280 (1997).
[14] R. Brun and F. Carminati, CERN Program Library Long Writeup W5013, 1993 (unpublished).
[15] S. Catani *et al.*, JHEP **0307**, 028 (2003).
[16] U. Aglietti *et al.*, arXiv:hep-ph/0610033 (2006).
[17] K.A. Assamagan *et al.*, arXiv:hep-ph/0406152 (2004).
[18] A. Djouadi, J. Kalinowski and M. Spira, Comput. Phys. Commun. **108**, 56 (1998).
[19] R. Hamberg, W.L. van Neerven and T. Matsuura, Nucl. Phys. **B359**, 343 (1991) [Erratum-ibid. **B644**, 403 (2002)].
[20] D. Acosta *et al.* (CDF collaboration), Phys. Rev. Lett. **95**, 022003 (2005).
[21] T. Binoth *et al.*, Eur. Phys. J. C. **16**, 311 (2000).
[22] J. Pumplin *et al.*, JHEP **0207**, 012 (2002).
[23] T. Junk, Nucl. Intrum. Methods A **434**, 435 (1999); A. Read, CERN 2000-005 (2000).
[24] W. Fisher, FERMILAB-TM-2386-E (2006).